



Trans. Nonferrous Met. Soc. China 22(2012) 157-163

Transactions of Nonferrous Metals Society of China

www.tnmsc.cn

Numerical calculation of flow field inside TiAl melt during rectangular cold crucible directional solidification

YANG Jie-ren, CHEN Rui-run, DING Hong-sheng, SU Yan-qing, HUANG Feng, GUO Jing-jie, FU Heng-zhi School of Materials Science and Engineering, Harbin Institute of Technology, Harbin 150001, China Received 23 September 2010; accepted 5 January 2011

Abstract: Numerical investigations on the flow field in Ti–Al melt during rectangular cold crucible directional solidification were carried out. Combined with the experimental results, 3-D finite element models for calculating flow field inside melting pool were established, the characteristics of the flow under different power parameters were further studied. Numerical calculation results show that there is a complex circular flow in the melt, a rapid horizontal flow exists on the solid/liquid interface and those flows confluence in the center of the melting pool. The flow velocity ν increases with the increase of current intensity, but the flow patterns remain unchanged. When the current is 1000 A, the ν_{max} reaches 4 mm/s and the flow on the interface achieves 3 mm/s. Flow patterns are quite different when the frequency changes from 10 kHz to 100 kHz, the mechanism of the frequency influence on the flow pattern is analyzed, and there is an optimum frequency for cold crucible directional solidification.

Key words: flow field; numerical calculation; TiAl alloys; cold crucible; directional solidification

1 Introduction

Electromagnetic cold crucible melting is a promising technology for melting reactive, high melting point and refractory materials. Combined with the directional solidification (DS), materials with oriented microstructure are prepared [1]. Due to the high specific strength, high temperature strength and exceptional high temperature creep resistance, Ti–Al alloys are considered one of the best potential blade materials in the next few decades [2]. Ti–Al alloys ingots with different compositions and sizes are prepared by cold crucible directional solidification [3].

Generally, solid/liquid (S/L) interface, superheat degree and flow pattern of the melt are the crucial factors that influence the microstructure during the whole DS process. In electromagnetic cold crucible, both the electromagnetic force on the melt and the stirring force inside the melt can influence the characteristics of the flow and the shape of the liquid melt. Flow would enhance the process of the heat transfer and the mass transfer inside the melting pool, this leads to the S/L interface concave and has an effect on the superheat. Furthermore, the continuity of the crystal growth is

disturbed. It is difficult to measure the flow pattern inside the melt pool of refractory or reactive metals in practice, especially for Ti-Al alloys in a small scale system.

Numerical simulations have already proved their potential in the investigation of the flow, the heat and species transfer in melting and solidification. In recent years, some investigations have been carried out on optimizing the crucible structure and calculating coupled field in the melt [4-6]. BAI [7] reported that there is a strong downstream flow along the surface and an upstream flow in the center, the flowing melt forms a complex circular pattern in the whole liquid meniscus. CHA et al [8] studied the flow field inside cold crucible melt by 3-D finite element method (FEM), and the results indicate that a swirling is presented in the melt and the melt near the slits flows upward. The flow velocity would be enhanced with the increase of the magnetic field intensity. It was reported a higher H/D ratio can improve superheat and homogenize the temperature inside the melt [9, 10]. Investigation on cylindrical crucible demonstrated that the material properties should be considered during the melting process [11].

During the process of cold crucible directional solidification, both the location of the S/L interface and

the shape of the liquid metal are critical factors that influence the flow pattern, but they are always neglected in previous works. Moreover, the flow fields are partly influenced by power parameters, such as the current intensity and the frequency. In this study, experiments of directional solidified Ti–Al alloys was carried out, then the S/L interface of the ingots were measured and the liquid meniscus shapes were restored. A 3-D numerical model considering the complex structure of the crucible was established. The flow fields were calculated and corresponding analyses were performed with different power parameters.

2 Experimental

The apparatus of cold crucible directional solidification is shown in Fig. 1. Cooling water was circulated in the crucible and the induction coil, and an adjustable AC was supplied into the coil. A liquid metal meniscus was formed on the base under the balance of hydrostatic pressure, magnetic pressure and the pressure caused by surface tension. When the superheat of the liquid reached some degree, the feeding of the raw rod and the withdrawal of the base started at the same time. Because of the strong cooling from the liquid alloys (Ga–In–Sn alloys) at the bottom, a higher longitudinal



 $\begin{tabular}{ll} Fig. 1 Photo of rectangular cold crucible system used for continuous melting and DS process \end{tabular}$

temperature gradient was set up, which was necessary for DS process. Hence, the melting and DS of Ti-Al alloys in the crucible was realized. The whole DS process is presented in Fig. 2.

The position of S/L interface and the meniscus shape were obtained by restoring the coil height, ingot length and bulk of the melt pool before and after the experiment. The ingot was cut along the broadside, polished and etched. The macrostructure of the S/L interface zone is shown in Fig. 3.

3 Numerical model and boundary conditions

3.1 Flow field equations

A 3-D numerical model was established according to the experimental prototype, and a quarter of the prototype was investigated due to its symmetry. The electromagnetic (EM) force and the flow field were carried out using the commercial program ANSYS (distributed by ANSYS HIT), where a self-developed FEM codes approach was used. The shape of meniscus was determined by the experimental measurement. The melt is considered the incompressible liquid, and the EM field and the flow field are decoupled. For FEM model, the physical characteristics of each component used for calculation are listed in Table 1. The velocities (ν) on free surface of melt satisfy the non-slip conditions:

$$v_x = v_y = v_z = 0 \tag{1}$$

The Navier-Stokes (N-S) equation is applied to the calculating domain, which can precisely characterize the 3-D flow and the distribution of pressure in the TiAl melt:

$$\rho \frac{\partial v}{\partial t} = \rho g - \nabla \cdot P + \mu \nabla^2 v \tag{2}$$

where ρ , P and μ are the density, pressure and viscosity of the fluid, respectively.

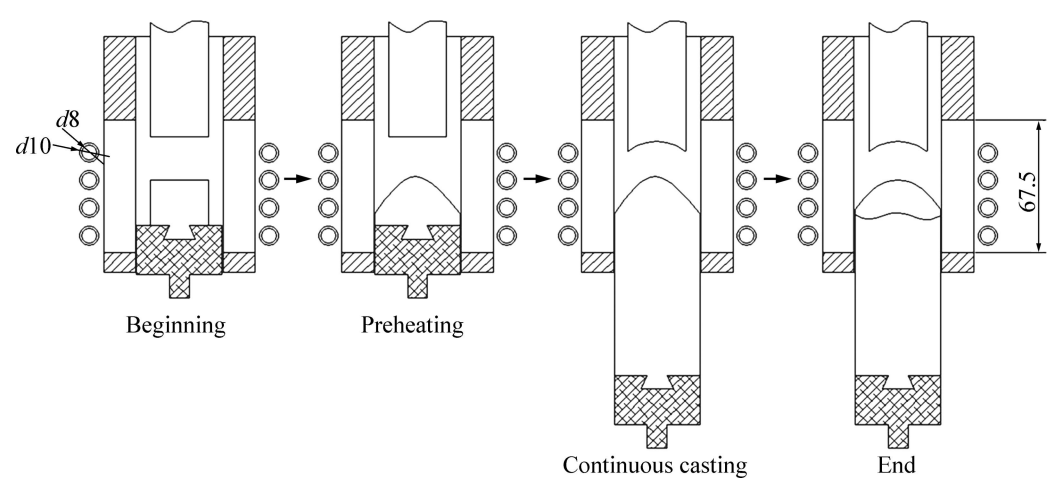


Fig. 2 Schematic diagram of DS process of Ti-Al alloy in cold crucible (Unit: mm)

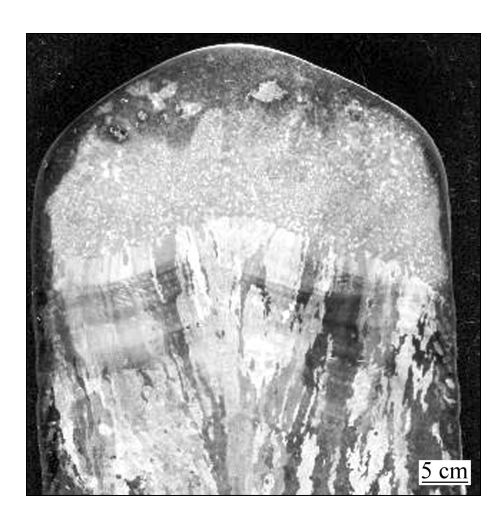


Fig. 3 Photo of S/L interface of Ti-Al ingot directionally solidified by cold crucible

Table 1 Physical properties of each component

Component	Relative magnetic permeability	Resistivity/ $(\Omega \cdot m)$	Viscosity/ (Pa·s)	Density/ (kg·m ⁻³)
TiAl alloy	1	1.79×10^{-6}	3	3780
Induction coil	1	1.67×10 ⁻⁸		
Cold crucible	1	1.67×10^{-8}		
Air	1			

3.2 Calculation model

To simplify the crucible model, mush zone and solid zone are taken as a whole region without flow. It is well known that melt would form meniscus under the EM force. In this study, the meniscus shape and its location were experimentally measured before and after directional solidification, the height was considered 20 mm, which were referred in finite element model, as seen in Fig. 4. It assumes that the S/L interface is an ideal planar which is in the middle of the first and the second coils, and the flow in front of S/L interface is only tangential. In addition, there is no normal movement of melt on the symmetry plane $(v_y \text{ is } 0 \text{ on } x-z \text{ plane} \text{ and } v_x \text{ is } 0 \text{ on } y-z \text{ plane})$. The total element number is 294862, and there are 19749 elements in the melting pool.

4 Results and discussion

4.1 Flow fields under different current intensities

The power with current intensities of 140, 300, 500 and 1000 A under 50 kHz was carried out separately. The magnetic force would be initially calculated and then exerted on the model of the melt pool.

Under the power of 140 A and 50 kHz, the calculated flow field in melt pool is shown in Fig. 5.

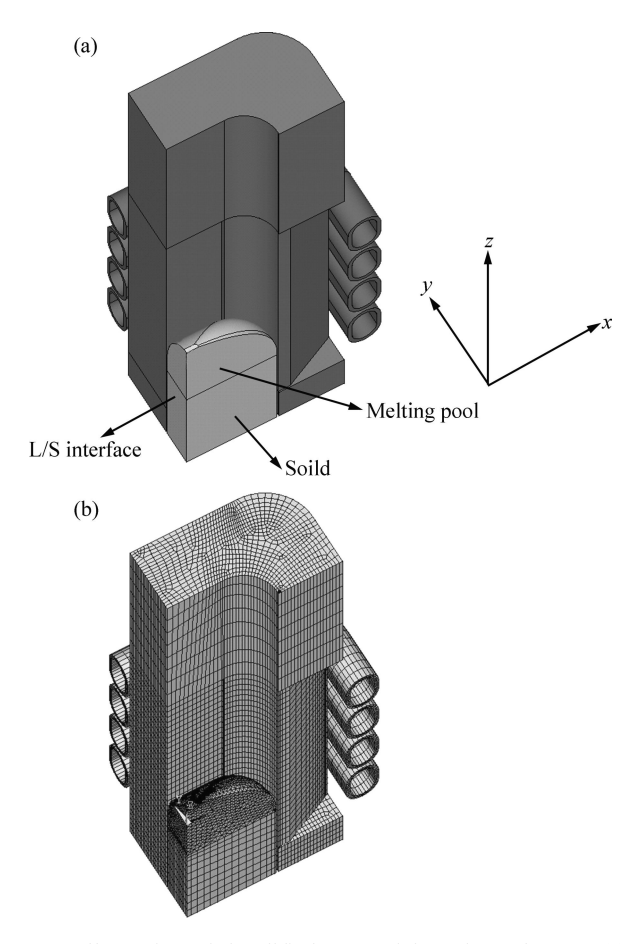


Fig. 4 Illustration of simplified FE models and FE element: (a) Crucible and sample model; (b) Finite element mesh

From Fig. 5, some of the melt near the corner flows forwards up intensively along the surface, then the flow shifts to clockwise gradually and turns to horizontal direction at the middle height of the meniscus, and then towards to the center. Subsequently, the flowing stream begins to flow apart, one small flow near the surface of the met reflows clockwise, the other larger flow continuously flows forwards down with decreasing velocity, and flows to the centre of S/L interface. In the view of that the model is one quarter of the crucible, the lateral flow near the S/L interface confluences each other in the center of the melt pool. Further, it flows into the reflow stream after a series of complex motions in the upper part of the meniscus. Evidently, the flow velocity near the S/L interface is higher than that in other regions, and the flow presents a rapid motion in the swirling region compared with the center, which can be clearly seen form Fig. 5. The flow velocity near the S/L interface reaches 0.15 mm/s.

The flow patterns under current intensities of 300, 500 and 1000 A are shown in Fig. 6, and Fig. 7 presents the flow velocities on the S/L interface in *x*-direction under different current intensities, as noted in Fig. 5(a). As shown in Fig. 6, the flow patterns remain unchanged

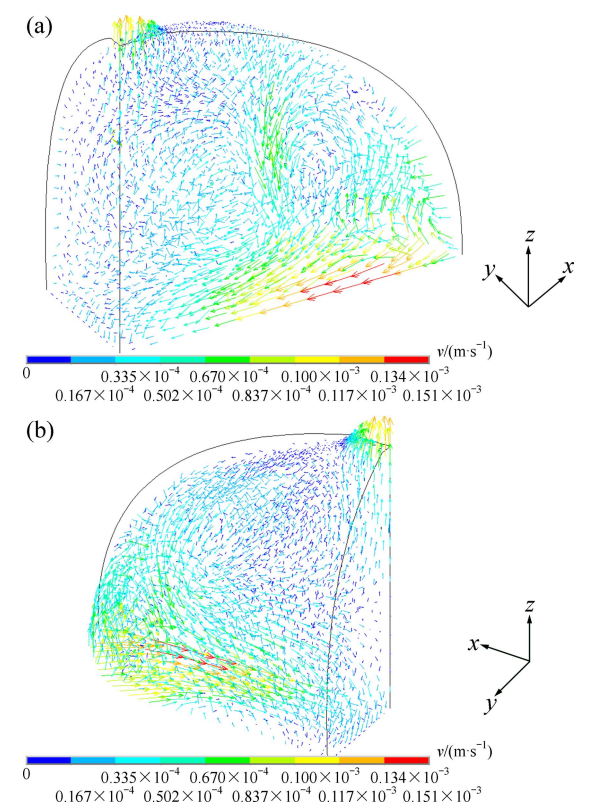


Fig. 5 Flow field of melt pool under 140 A and 50 kHz: (a) Inside; (b) Outside

with the increase of the current intensity under the same frequency. However, the flow velocity increases with the increase of current intensity. Under the current of 300 and 500 A, the liquid near the S/L interface flows to the center of the melt and the $v_{\rm max}$ reaches 0.7 and 2 mm/s, respectively. Under the current of 1000 A, the flow velocity increases obviously, the $v_{\rm max}$ reaches 4 mm/s and the flow on the interface achieves 3 mm/s.

The flow pattern in the melt has a significant effect macro-segregation and micro-structural on morphology in DS process [12-15]. The convection in small ceramic tubes (the diameter is in the range of 0.6–6 mm) originating from solute separation and temperature gradient increases with the increase of the diameter, and the double-diffusion layer appears along the longitudinal direction in the front of S/L interface [16, 17]. As for some materials such as Sn-Cd alloys, the S/L interface would curve due to the wall-effect [18], and the dendrite or cellular crystal grows toward the flow direction [19, 20], which would directly change the morphology of S/L interface. Moreover, the convection would cause the solute redistribute around the dendrite tip which causes the nonuniformity of the constitutional super cooling.

For small diameter samples, the influence of convection on the crystal growth is generally omitted, investigations on the evolving of macro- and micro-structure and the morphology of S/L interface have been carried out [21, 22]. Whereas, the convection

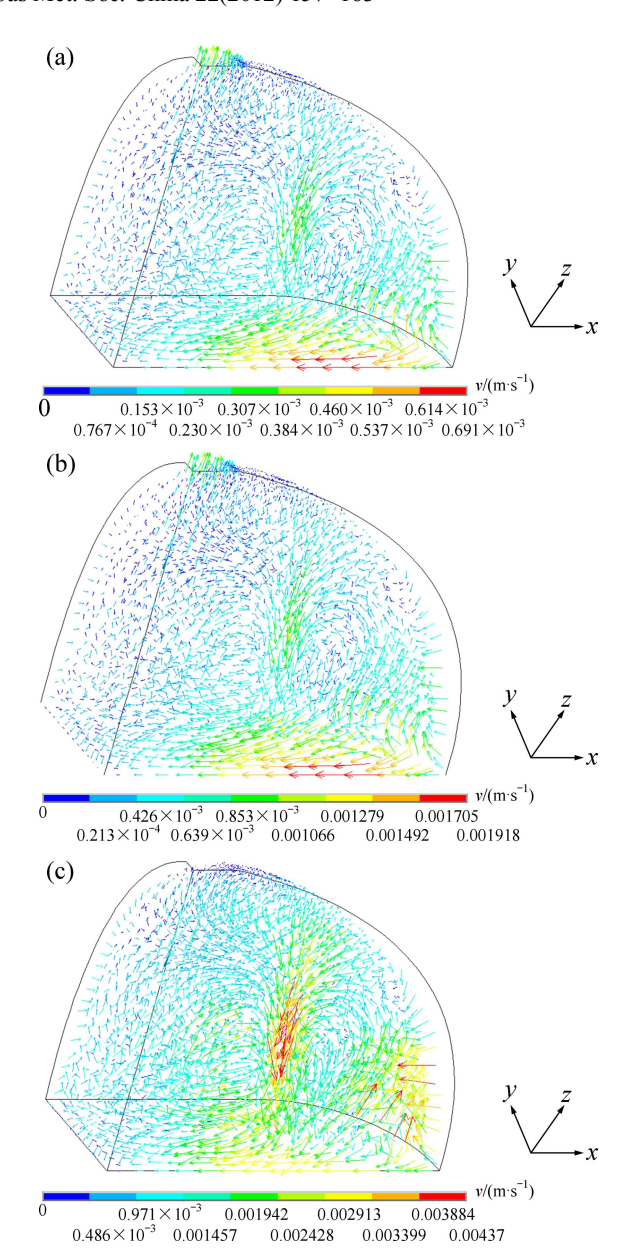


Fig. 6 Flow fields under different intensities with 50 kHz: (a) 300 A; (b) 500 A; (c) 1000 A

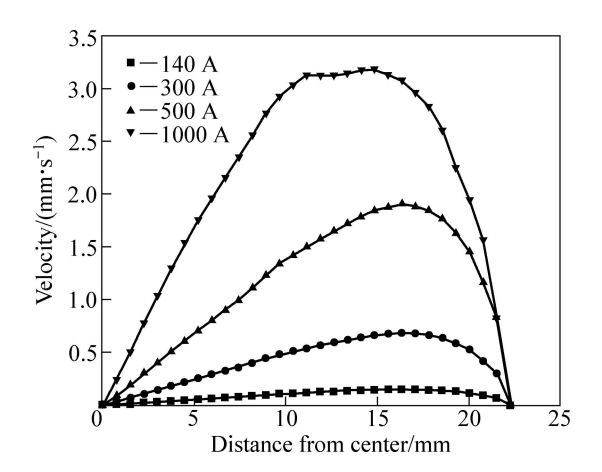


Fig. 7 Flow velocities on S/L interface in x-direction under different current intensities

is very obvious in rectangular cold crucible, and the convection in melt cannot be neglected in the engineering fabrication during DS process. There is obvious difference for the DS process with or without forced convection. As depicted above, the forced convection resulting from electromagnetic force in bulky melt is much complicated and has an evident effect on the crystal growth. An evident phenomenon occurring in cold crucible directional solidification is that the forced convection induced by EM stirring would promote columnar to equiaxed transformation, and then the columnar crystal growth is disturbed [23].

4.2 Flow fields under different frequencies

Flow fields are calculated when the current intensity is 1000 A and the frequency is 10, 20, 50 and 100 kHz, respectively, the results are shown in Fig. 8. The skin depth is calculated as

$$S = \frac{1}{\sqrt{\pi f \mu \sigma}} \tag{3}$$

where δ is the skin depth, f is the power frequency, μ is the magnetic permeability and σ is the conductivity. According to Eq. (3), the penetration of magnetic field increases with the decrease of the power frequency. Consequently, the whole flow pattern changes in the expanded region of electromagnetic stirring.

The change of power frequency influences the flow field on two aspects. On one hand, the increased frequency reduces both the penetration of magnetic field and the stirring force, and the decreased stirring force cannot completely overcome the viscous force of the melt. Therefore, this is not good for the homogenization of the heat and the mass inside the melt. On the other hand, the increased frequency enhances the constraint force on the melt and that is beneficial to the soft-contact between the melt and the crucible inner wall. Since that, there is an optimum frequency under a specific power for melting and DS process.

A simple circular flow is presented in cylindrical crucible [10]. In contrast, a complex flow is presented in the melt during the DS process by rectangular cold crucible.

The change of the flow patterns can be clearly presented on the x-z plane, as shown in Fig. 9. There is a clockwise swirl inside the melt pool and an upper steam near the top of the meniscus for all fields. However, those flow patterns are quite different when the frequency changes from 10 to 100 kHz. Under a lower frequency, the circulation region is more extensive and the flow vortex is much closer to the center, as seen in Figs. 8(a), 8(b), 9(a) and 9(b). When the frequency is higher, the swirl pattern inside the melt pool disappears gradually, as seen in Figs. 8(c), 8(d), 9(a) and 9(d). Figure 10 presents the flow velocities on S/L interface in *x*-direction under different current frequencies. Compared with Fig. 7, it can be found form Fig. 10 that the effect of current frequency on flow velocity on S/L interface is complicated.

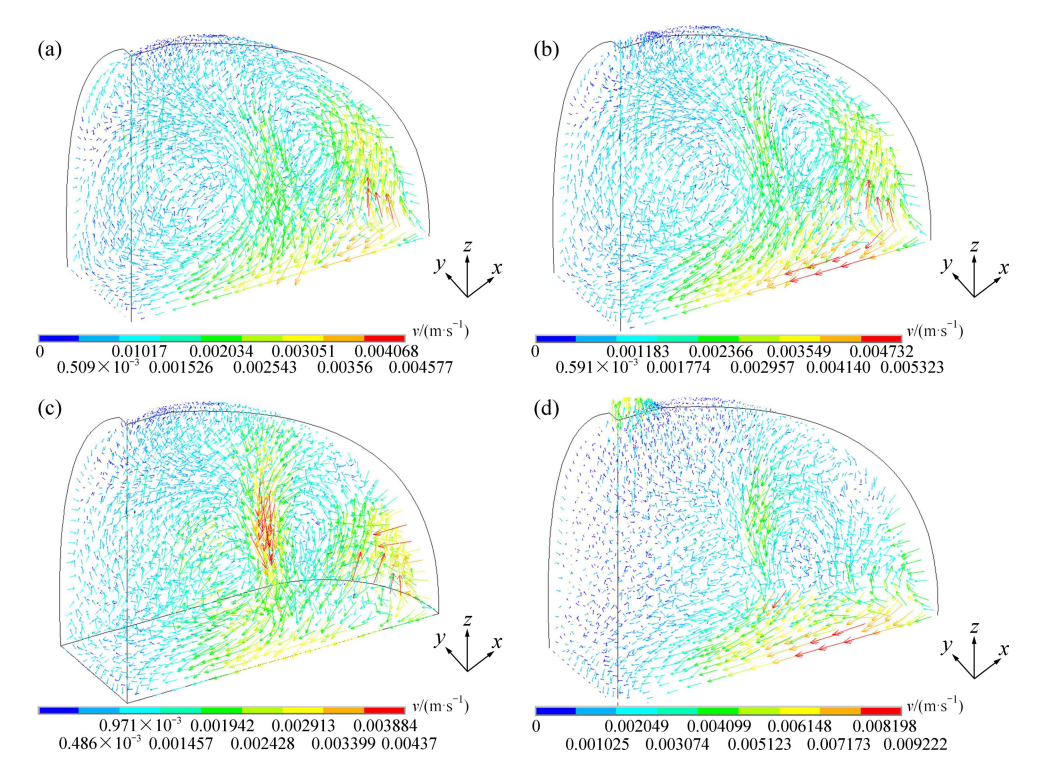


Fig. 8 Flow fields under 1000 A with different frequencies: (a) 10 kHz; (b) 20 kHz; (c) 50 kHz; (d) 100 kHz

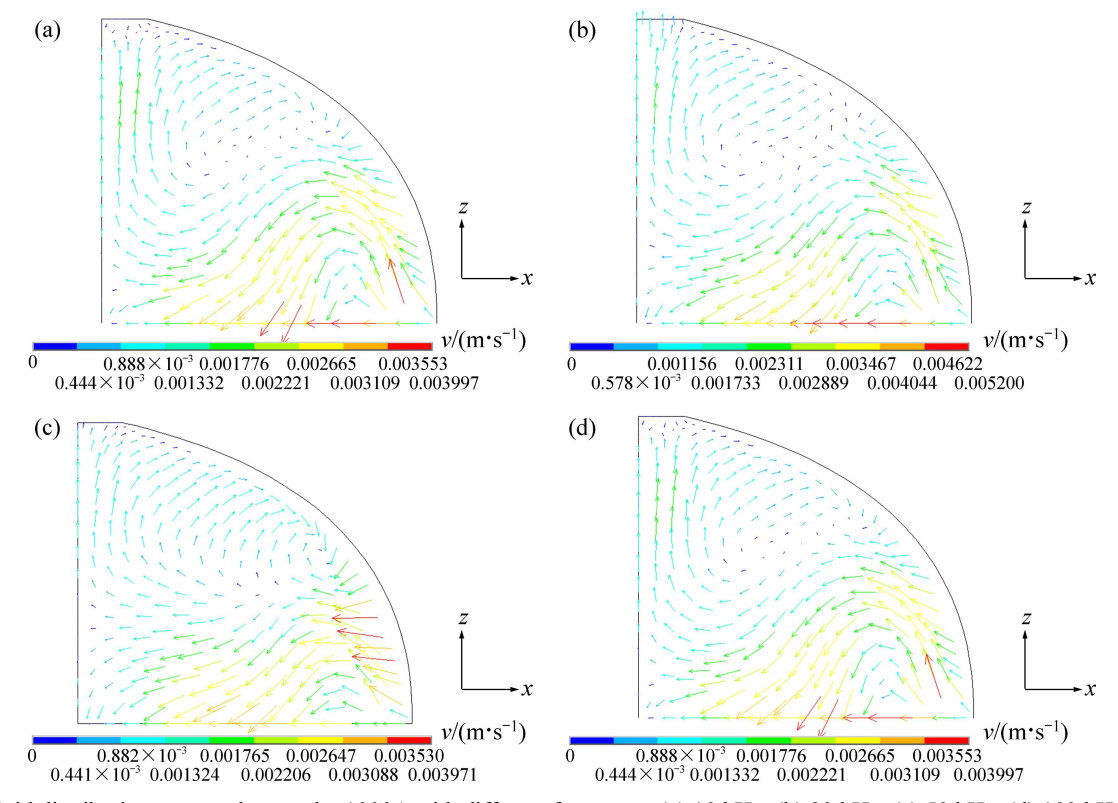


Fig. 9 Fluid distribution on x-z plane under 1000A with different frequency: (a) 10 kHz; (b) 20 kHz; (c) 50 kHz; (d) 100 kHz

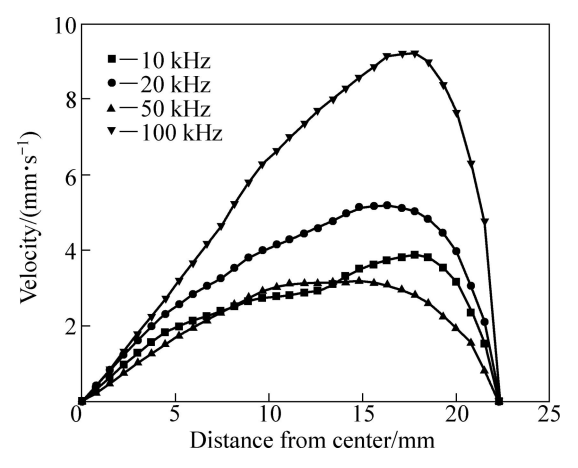


Fig. 10 Flow velocities on S/L interface in *x*-direction under different current frequency

5 Conclusions

- 1) A 3-D rectangular cold crucible model is established and calculated in directionally solidifying Ti–Al alloys under different current intensities and frequencies based on the experimental results.
- 2) There is a complex circular flow in the melt pool, a swirling flow arises near the crucible corner and a rapid horizontal flow on the S/L interface, and those flows confluence each other in the center of the melt pool.
 - 3) The flow velocity increases with the increase of

current intensity from 140 to 1000 A, whereas, the flow patterns remain unchanged. Under the current of 1000 A, the $v_{\rm max}$ reaches 4 mm/s and the flow on the interface achieves 3 mm/s.

4) Under a lower frequency, the region of electromagnetic stirring is more extensive and the swirling flow is much closer to the center. When the frequency is higher, the swirling pattern inside the melt pool disappears gradually. There is an optimum frequency for melting and DS process.

References

- [1] CHEN Rui-run, DING Hong-sheng, GUO Jing-jie, BI Wei-sheng, FU Heng-zhi. Continuous and directional solidification technology of titanium alloys with cold crucible [J]. Transactions of Nonferrous Metals Society of China, 2006, 16(S2): s154-s159.
- [2] LU Yong-hao, ZHANG Yong-gang, QIAO Li-jie, WANG Yan-bin, CHEN Chang-qi, CHU Wu-yang. In-situ crack propagation observation in fully lamellar Ti-49%Al alloy [J]. Transactions of Nonferrous Metals Society of China, 2000, 10(5): 599-602.
- [3] FU Heng-zhi, DING Hong-sheng, CHEN Rui-run. Directional solidification technology based on electromagnetic cold crucible to prepare TiAl intermetallics [J]. Rare Metal Materials and Engineering, 2008, 37(4): 565-570.
- [4] CHO Y W, OH Y J, YI K W. Numerical analysis of molten metal shape in cold crucibles by 3D FEM [J]. Modeling and Simulation in Materials Science and Engineering, 1996, 4(1): 11–22.
- [5] DENG Kang, ZHOU Yue-ming, REN Zhong-ming, GONG Tao, JIANG Guo-chang. Electromagnetic characteristics of levitation melting with cold crucible [J]. Transactions of Nonferrous Metals

- Society of China, 1999, 9(2): 387-392.
- [6] KAWASE Y, YOSHIDA T. 3-D finite element analysis of molten metal shape in rectangular cold crucible system [J]. IEEE Transactions on Magnetics, 1999, 35(3): 1889–1892.
- BAI Yun-feng. Numerical calculation and transmission coupling model in cold crucible directional solidification of Ti alloys [D].
 Harbin: Harbin Institute of Technology, 2006: 127–129. (in Chinese)
- [8] CHA P R, HWANG Y S, OH Y J. Numerical analysis on cold crucible using 3-D H—φ method and finite volume method with non-staggered BFC grid system [J]. ISIJ International, 1996, 36(9): 1157–1165.
- [9] BAAKE E, NACKE B, BERNIER F. Experimental and numerical investigations of the temperature field and melt flow in the induction furnace with cold crucible [J]. Compel: The International Journal For Computation and Mathematics in Electrical and Electronic Engineering, 2003, 22(1): 88-97.
- [10] UMBRASKO A, BAAKE E, NACKE B. Numerical studies of the melting process in the induction furnace with cold crucible [J]. Compel: The International Journal for Computation and Mathematics in Electrical and Electronic Engineering, 2008, 27(2): 359–368.
- [11] PERICLEOUS K, BOJAREVICS V, DJAMBAZOV G. Experimental and numerical study of the cold crucible melting process [J]. Applied Mathematics Modeling, 2006, 30(11): 1262–1280.
- [12] HU Xiao-wu, LI Shuang-ming, GAO Si-feng. Effect of melt convection on primary dendrite arm spacing in directionally solidified Pb–26%Bi hypo-peritectic alloys [J]. Transactions of Nonferrous Metals Society of China, 2011, 21(1): 65–71.
- [13] KARTAVYKH A, GINKIN V, GANINA S. Numerical study of convection-induced peritectic macro-segregation effect at the directional counter-gravity solidification of Ti-46Al-8Nb alloy [J]. Intermetallics, 2011, 19(6): 769-775.
- [14] YANG Wan-hong, CHANG K M, CHEN Wei, MANNAN S, DEBARBADILLO J. Freckle criteria for the upward directional solidification of alloys [J]. Metallurgical and Materials Transactions A, 2001, 32(4): 397–406.

- [15] CHEN J, SUNG P K, TEWARI S N, POIRIER D R, DEGROH H C. Directional solidification and convection in small diameter crucibles [J]. Materials Science and Engineering A, 2003, 357(1-2): 397-405.
- [16] TRIVEDIA R, MIYAHARA H, MAZUMDER P, SIMSEK E, TEWARI S N. Directional solidification microstructures in diffusive and convective regimes [J]. Journal of Crystal Growth, 2001, 222(1-2): 365-379.
- [17] SU Yan-qing, LI Xin-zhong, GUO Jing-jie. Phase and microstructure selection in directionally solidified peritectic alloys with convection [J]. Transactions of Nonferrous Metals Society of China, 2006, 16(S2): s53-s58.
- [18] TRIVEDIA R, MAZUMDER P, TEWARI S N. The effect of convection on disorder in primary cellular and dendritic arrays [J]. Metallurgical and Materials Transactions A, 2002, 33(12): 3763-3775.
- [19] NOEPPEL A, CIOBANAS A, WANG X D. Influence of forced/natural convection on segregation during the directional solidification of Al-based binary alloys [J]. Metallurgical and Materials Transactions B, 2010, 41(1): 193–208.
- [20] LIU Shan, LU De-yang, HUANG Tao. Study on the formation and structure of spike-like crystals [J]. Materials Science and Technology, 1992, 11(2): 75–80.
- [21] KARTAVYKH A, GINKIN V, GANINA S. Convection-induced peritectic macro-segregation proceeding at the directional solidification of Ti-46Al-8Nb intermetallic alloy [J]. Materials Chemistry and Physics, 2011, 126(1-2): 200-206.
- [22] CHEN J, TEWARI S N, MAGADI G, DeGROH H C. Effect of crucible diameter reduction on the convection, macrosegregation, and dendritic morphology during directional solidification of Pb-2.2 wt pct Sb alloy [J]. Metallurgical and Materials Transactions A, 2003, 34(12): 2985–2990.
- [23] YANG Jie-ren, CHEN Rui-run, DING Hong-sheng, GUO Jing-jie, FU Heng-zhi. Columnar crystal growth of Ti-46Al-0.5W-0.5Si alloys directional solidified by rectangular cold crucible [J]. Advanced Materials Research, 2011, 154-155: 743-751.

矩形冷坩埚定向凝固过程中钛铝熔体的流场数值计算

杨劼人,陈瑞润,丁宏升,苏彦庆,黄锋,郭景杰,傅恒志

哈尔滨工业大学 材料科学与工程学院,哈尔滨 150001

摘 要:对矩形冷坩埚定向凝固钛铝合金熔体流场开展数值模拟研究。结合实验结果,建立熔体流场的 3-D 有限元模型,研究不同电源参数下熔池内流动特性。计算结果表明:熔池内存在着复杂的循环流动,在固液界面前端存在着较为强烈的径向对流,并在中部合流。熔体流动随着电流强度的增强而增强,但是宏观流动形貌并没有改变。当电流为 1000 A 时,熔池内最大流速为 4 mm/s,固-液界面前端达到 3 mm/s。当频率从 10 kHz 变化到 100 kHz 时,熔池流动形貌发生明显改变,分析其影响机制。对于冷坩埚定向凝固,存在着一个最佳频率。

关键词: 流场: 数值计算: 钛铝合金: 冷坩埚: 定向凝固

(Edited by FANG Jing-hua)